Synthesis and Characterization of Pt Dendrimer-Encapsulated Nanoparticles: Effect of the Template on Nanoparticle Formation

Marc R. Knecht,[†,⊥] Michael G. Weir,[†] V. Sue Myers,[†] William D. Pyrz,[‡] Heechang Ye,[†] Valeri Petkov,*[,§] Douglas J. Buttrey,*[,‡] Anatoly I. Frenkel,*[,||] and Richard M. Crooks*[,†]

Department of Chemistry and Biochemistry, Texas Materials Institute, Center for Nano- and Molecular Science and Technology, The University of Texas at Austin, 1 University Station, A5300, Austin, Texas 78712-0165, Center for Catalytic Science and Technology, Department of Chemical Engineering, University of Delaware, Newark, Delaware 19716, Department of Physics, 203 Dow Science, Central Michigan University, Mt. Pleasant, Michigan 48859, and Department of Physics, Yeshiva University, 245 Lexington Avenue, New York, New York 10016

Received February 11, 2008. Revised Manuscript Received June 10, 2008

In this article, we provide a detailed description of the synthesis and properties of Pt dendrimer-encapsulated nanoparticles (DENs) prepared using sixth-generation, hydroxyl-terminated, poly(amidoamine) (PAMAM) dendrimers (G6−OH) and three different $PtCl_4^{2-}$/G6−OH ratios: 55, 147, and 240. Results obtained from UV−vis spectroscopy, X-ray photoelectron spectroscopy, electron microscopy, X-ray absorption spectroscopy, and high-energy X-ray diffraction show that only a fraction of the Pt^{2+}/dendrimer precursors are reduced by BH_4^- and that the reduction process is highly heterogeneous. That is, after reduction each Pt^{2+}/dendrimer precursor complex is either fully reduced, to yield a DEN having a size and structure consistent with the original $PtCl_4^{2-}$/dendrimer ratio used for the synthesis, or the precursor is not reduced at all. This result is consistent with an autocatalytic process that entails slow formation of a nascent catalytic Pt seed within the dendrimer, followed by rapid, catalytic reduction of nearby Pt^{2+} ions. Details concerning the formation of the Pt^{2+}/dendrimer precursor are also discussed.

Introduction

We report the atomic-level physical characterization of Pt dendrimer-encapsulated nanoparticles (DENs)[1] with an emphasis on the relationship between the Pt^{2+}/dendrimer composite starting material and the structural properties of the corresponding DENs. Here, Pt^{2+} refers to any form of Pt^{2+} regardless of its ligand field. This is a timely study, because it has recently been found that the use of slightly different synthetic methods for preparing Pt DENs leads to different products.[2–5] The purpose of this paper is to reconcile these reports using a combination of time-resolved UV−vis spectroscopy, X-ray photoelectron spectroscopy (XPS), high-resolution transmission electron microscopy (HRTEM), extended X-ray absorption fine structure (EXAFS) spectroscopy, and high-energy X-ray diffraction (XRD) coupled with pair-distribution function (PDF) analysis. The combination of these analytical methods, which provide complementary information, is important because DENs are good models for studying the effect of nanoparticle size, composition, and structure on catalytic activity.[6–17] However, to extract useful correlations of this sort, it is necessary that there be consensus on the DEN structure.

The key findings of this study are as follows. First, time-resolved UV−vis spectroscopy indicates that the Pt species required for dendrimer binding is $PtCl_n(H_20)_{4-n}^{2-n}$, where $n \leq 3$. Second, the UV−vis and XPS data indicate that reduction of the Pt^{2+}/dendrimer complexes with BH_4^- is incomplete. Third, EXAFS results indicate relatively low Pt−Pt coordination numbers (CNs) that are consistent with

* To whom correspondence should be addressed. E-mail: crooks@cm.utexas.edu (R.M.C.); dbuttrey@udel.edu (D.J.B.); petkov@phy.cmich.edu (V.P.); anatoly.frenkel@yu.edu (A.I.F.). Phone: 512-475-8674(R.M.C.); 302-831-2034(D.J.B.); 989-774-3395(V.P.); 212-340-7827(A.I.F.).
† The University of Texas at Austin.
‡ University of Delaware.
§ Central Michigan University.
|| Yeshiva University.
⊥ Present address: Department of Chemistry, University of Kentucky, 125 Chemistry Physics Building, Lexington, KY 40506.

(1) Scott, R. W. J.; Wilson, O. M.; Crooks, R. M. *J. Phys. Chem. B* **2005**, *109*, 692–704.
(2) Ye, H.; Scott, R. W. J.; Crooks, R. M. *Langmuir* **2004**, *20*, 2915–2920.
(3) Ye, H.; Crooks, R. M. *J. Am. Chem. Soc.* **2005**, *127*, 4930–4934.
(4) Ozturk, O.; Black, T. J.; Perrine, K.; Pizzolato, K.; Williams, C. T.; Parsons, F. W.; Ratliff, J. S.; Gao, J.; Murphy, C. J.; Xie, H.; Ploehn, H. J.; Chen, D. A. *Langmuir* **2005**, *21*, 3998–4006.
(5) Alexeev, O. S.; Siani, A.; Lafaye, G.; Williams, C. T.; Ploehn, H. J.; Amiridis, M. D. *J. Phys. Chem. B* **2006**, *110*, 24903–24914.
(6) Garcia-Martinez, J. C.; Lezutekong, R.; Crooks, R. M. *J. Am. Chem. Soc.* **2005**, *127*, 5097–5103.
(7) Hoover, N. N.; Auten, B. J.; Chandler, B. D. *J. Phys. Chem. B* **2006**, *110*, 8606–8612.
(8) Narayanan, R.; El-Sayed, M. A. *J. Phys. Chem. B* **2004**, *108*, 8572–8580.
(9) Niu, Y.; Yeung, L. K.; Crooks, R. M. *J. Am. Chem. Soc.* **2001**, *123*, 6840–6846.
(10) Scott, R. W. J.; Wilson, O. M.; Oh, S.-K.; Kenik, E. A.; Crooks, R. M. *J. Am. Chem. Soc.* **2004**, *126*, 15583–15591.
(11) Wilson, O. M.; Knecht, M. R.; Garcia-Martinez, J. C.; Crooks, R. M. *J. Am. Chem. Soc.* **2006**, *128*, 4510–4511.
(12) Chandler, B. D.; Gilbertson, J. D. *Top. Organomet. Chem.* **2006**, *20*, 97–120.
(13) Vijayaraghavan, G.; Stevenson, K. J. *Langmuir* **2007**, *23*, 5279–5282.
(14) Ye, H.; Crooks, R. M. *J. Am. Chem. Soc.* **2007**, *129*, 3627–3633.
(15) Korkosz, R. J.; Gilbertson, J. D.; Prasfika, K. S.; Chandler, B. D. *Catal. Today* **2007**, *122*, 370–377.
(16) Ye, H.; Crooks, J. A.; Crooks, R. M. *Langmuir* **2007**, *23*, 11901–11906.
(17) Astruc, D. *Nanoparticles and Catalysis*; Wiley: New York, 2007.

10.1021/cm8004198 CCC: $40.75
Published on Web 07/30/2008

the UV−vis and XPS data. Fourth, HRTEM and XRD/PDF analyses indicate that Pt DENs possess a face-centered cubic (fcc)-type structure and sizes that correlate very well to the initial $PtCl_4^{2-}$/dendrimer ratio used for the synthesis. To summarize, results obtained from TEM and XRD/PDF indicate the presence of fully reduced Pt DENs, whereas UV−vis, XPS, and EXAFS spectroscopic data are consistent with incomplete reduction of the Pt^{2+}/dendrimer precursors. Here we show how these seemingly inconsistent results can be unified with a single model that invokes a bimodal distribution of products.

The DEN synthesis is carried out in two steps. First, metal ions are introduced to a solution of dendrimers, which results in complexation of the ions with interior tertiary amines of the dendrimer. Second, the encapsulated metal ions are chemically reduced, which usually results in formation of zerovalent DENs. With the use of this method, monometallic DENs (Au, Pd, Pt, Cu, Ag, Ni, and Fe),[1,13,15,18–26] bimetallic alloy and core−shell DENs (PdPt, PdAu, AuAg, and PtCu),[7,10,12,27–30] and semiconducting quantum dots (CdS) have been prepared.[31] These materials, which range in size from just a few atoms[32,33] to perhaps 1000 atoms, are often nearly monodisperse in size, composition, and structure.[6–13,34,35] Moreover, because the dendrimers are highly permeable and do not passivate the surface of the encapsulated nanoparticles, DENs are also good model catalysts.[1,6,12]

There are some interesting differences between Pt DENs and other monometallic DENs.[3,5,34] Most notably, the Pt DEN synthesis requires a significantly longer period of time to complete (∼4 days) compared to other types of DENs (typically ∼1 h).[18,19] On the basis of several recent reports, we believe the rate-limiting process in the DEN synthesis is complexation between Pt^{2+} and tertiary amines within the dendrimer.[2,4,5,34,36] $PtCl_4^{2-}$ is typically the source of Pt^{2+} for the synthesis of Pt DENs, and in this case the complexation process likely involves two steps: hydrolysis of one or more Pt−Cl bonds followed by Pt−amine bond formation. Pellechia et al. have reported NMR data suggesting the presence of numerous mono- and bidentate binding motifs between Pt^{2+} and sites within second- and fourth-generation, hydroxyl-terminated poly(amidoamine) (PAMAM) dendrimers (G2−OH and G4−OH, respectively).[36] We believe their model is generally correct, but they did not invoke the $PtCl_4^{2-}$ hydrolysis step which we will show here to be a requirement for complexation. Indeed, this sequence of reactions (Pt−Cl bond hydrolysis followed by reaction with an amine) has been previously observed for related compounds.[37,38] Recent EXAFS results from Alexeev et al. have provided support for the NMR results.[5] This group also studied the reactivity of $PtCl_4^{2-}$ with water in the absence of dendrimer and interpreted the results in terms of hydrolysis of two Pt−Cl bonds.[5]

Another aspect of the Pt DEN synthesis that distinguishes it from other types of DENs is that a larger excess of reductant (BH_4^-) is required and that the reduction must be carried out in a sealed container.[3] These requirements are necessary to ensure that a partial pressure of H_2, which is a byproduct of the aqueous BH_4^- reduction step, is retained within the reaction vessel. In solutions saturated with N_2 or air, conversion of the Pt^{2+}/dendrimer complexes to zerovalent DENs does not occur.[5] However, even when the reduction is carried out under favorable conditions, we[2] and others[4] have observed that complete reduction of intradendrimer Pt^{2+} may still not take place. For example, the positions of the Pt($4f_{7/2}$) peaks in XPS spectra are shifted positive from the positions corresponding to zerovalent, bulk Pt. Such shifts may correspond to the presence of unreduced Pt^{2+} [4] or from quantum effects associated with these very small metal nanoparticles.[2,39–41]

In this article, we provide a detailed description of the synthesis and properties of Pt DENs prepared using sixth-generation, hydroxyl-terminated, PAMAM dendrimers (G6−OH) and three different $PtCl_4^{2-}$/G6−OH ratios: 55, 147, and 240. Our principal finding is that only a fraction of the total number of Pt^{2+} ions encapsulated within the dendrimers is reduced, but that the reduction process is highly heterogeneous. In other words, after reduction each Pt^{2+}/dendrimer precursor is either fully reduced, to yield a DEN having a size and structure consistent with the original $PtCl_4^{2-}$/dendrimer ratio used for the synthesis, or the precursor is not reduced at all. That is, the product resulting from exposure to BH_4^- is a bimodal mixture of precursor that is fully reduced and precursor that is not reduced at all (Scheme 1). This counterintuitive result is consistent with an autocatalytic process that entails slow formation of a nascent catalytic Pt seed within the dendrimer, followed by rapid, catalytic reduction of nearby Pt^{2+} ions.

(18) Zhao, M.; Sun, L.; Crooks, R. M. *J. Am. Chem. Soc.* **1998**, *120*, 4877–4878.
(19) Scott, R. W. J.; Ye, H.; Henriquez, R. R.; Crooks, R. M. *Chem. Mater.* **2003**, *15*, 3873–3878.
(20) Knecht, M. R.; Garcia-Martinez, J. C.; Crooks, R. M. *Chem. Mater.* **2006**, *18*, 5039–5044.
(21) Knecht, M. R.; Crooks, R. M. *New J. Chem.* **2007**, *31*, 1349–1353.
(22) Kim, Y.-G.; Oh, S.-K.; Crooks, R. M. *Chem. Mater.* **2004**, *16*, 167–172.
(23) Gröhn, F.; Bauer, B. J.; Akpalu, Y. A.; Jackson, C. L.; Amis, E. J. *Macromolecules* **2000**, *33*, 6042–6050.
(24) Mark, S. S.; Bergkvist, M.; Yang, X.; Angert, E. R.; Batt, C. A. *Biomacromolecules* **2006**, *7*, 1884–1897.
(25) Zhu, H.; Zhu, Y.; Yang, X.; Li, C. *Chem. Lett.* **2006**, *35*, 326–327.
(26) Tran, M. L.; Zvyagin, A. V.; Plakhotnik, T. *Chem. Commun.* **2006**, *2006*, 2400–2401.
(27) Knecht, M. R.; Weir, M. G.; Frenkel, A. I.; Crooks, R. M. *Chem. Mater.* **2008**, *20*, 1019–1028.
(28) Scott, R. W. J.; Datye, A. K.; Crooks, R. M. *J. Am. Chem. Soc.* **2003**, *125*, 3708–3709.
(29) Scott, R. W. J.; Sivadinarayana, C.; Wilson, O. M.; Yan, Z.; Goodman, D. W.; Crooks, R. M. *J. Am. Chem. Soc.* **2005**, *127*, 1380–1381.
(30) Wilson, O. M.; Scott, R. W. J.; Garcia-Martinez, J. C.; Crooks, R. M. *J. Am. Chem. Soc.* **2005**, *127*, 1015–1024.
(31) Lemon, B. I.; Crooks, R. M. *J. Am. Chem. Soc.* **2000**, *122*, 12886–12887.
(32) Zheng, J.; Dickson, R. M. *J. Am. Chem. Soc.* **2002**, *124*, 13982–13983.
(33) Zheng, J.; Petty, J. T.; Dickson, R. M. *J. Am. Chem. Soc.* **2003**, *125*, 7780–7781.
(34) Zhao, M.; Crooks, R. M. *Angew. Chem., Int. Ed.* **1999**, *38*, 364–366.
(35) Yeung, L. K.; Crooks, R. M. *Nano Lett.* **2001**, *1*, 14–17.
(36) Pellechia, P. J.; Gao, J.; Gu, Y.; Ploehn, H. J.; Murphy, C. J. *Inorg. Chem.* **2004**, *43*, 1421–1428.
(37) Lippard, S. J.; Berg, J. M. *Principals of Bioinorganic Chemistry*; 1st ed.; University Science Books: Mill Valley, CA, 1994.
(38) Rochon, F. D.; Fleurent, L. *Inorg. Chim. Acta* **1988**, *143*, 81–87.
(39) Fu, X.; Wang, Y.; Wu, N.; Gui, L.; Tang, Y. *J. Colloid Interface Sci.* **2001**, *243*, 326–330.
(40) Eberhardt, W.; Fayet, P.; Cox, D. M.; Fu, Z.; Kaldor, A.; Sherwood, R.; Sondericker, D. *Phys. Rev. Lett.* **1990**, *64*, 780–783.
(41) You, T.; Niwa, O.; Horiuchi, T.; Tomita, M.; Iwasaki, Y.; Ueno, Y.; Hirono, S. *Chem. Mater.* **2002**, *14*, 4796–4799.

Scheme 1

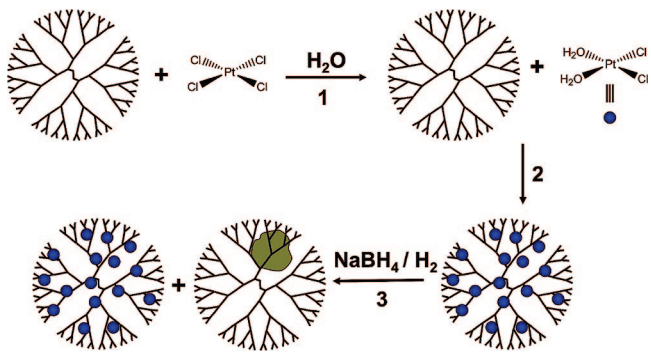

Experimental Section

Chemicals. G6−OH dendrimers were purchased from Dendritech, Inc. (Midland, MI) as 10.0 wt % solutions in MeOH. Prior to use, the dendrimer stock solution was dried under vacuum and then redissolved in sufficient deionized water to make a 100 μM solution. The K_2PtCl_4, $NaBH_4$, and KCl were purchased from Sigma-Aldrich (Milwaukee, WI) and used as received. Aqueous solutions were prepared using 18 MΩ·cm Milli-Q water (Millipore, Bedford, MA).

Synthesis of Pt DENs. Pt DENs were prepared using previously described methods.[3] Briefly, an aqueous solution of G6−OH was prepared. To this solution, 55, 147, or 240 equiv of a freshly prepared 100 mM K_2PtCl_4 aqueous solution was added to yield the G6−OH$(Pt^{2+})_n$ (n = 55, 147, or 240) Pt^{2+}/dendrimer complexes, respectively. Unless otherwise indicated, the solutions were allowed to stir for 3.0 days to ensure complete complexation of Pt^{2+} to the tertiary amines present within the dendrimer interior. Note that there are 254 tertiary amines within G6−OH. These precursor complexes were then reduced using at least a 10-fold molar excess of $NaBH_4$ from a freshly prepared aqueous 0.50 M stock solution. The final concentration of dendrimer in all cases was 10.0 μM. Reduction was allowed to proceed for 24.0 h in a sealed reaction vessel prior to subsequent analysis. Powder samples of the DENs were obtained by lyophilization (Freezone 12, Labconco Corp.).

Characterization. UV−vis spectra were obtained using a photodiode array UV−vis spectrometer (model 8453, Agilent Technologies) and 1.00 or 0.200 cm quartz cuvettes. All spectra were background-corrected using a spectrum obtained from an aqueous 10.0 μM dendrimer solution. XPS data were collected using a Kratos Axis Ultra DLD spectrometer having a monochromatic Al Kα X-ray source. Spectra were collected in charge-compensation mode at a pass energy of 20 eV, a resolution of 0.1 eV, and a dwell time of 1.00 s. The samples were prepared by submerging Au-coated Si wafers in a freshly prepared 10.0 μM DEN solution for 3.0 h.[42] The DEN-modified wafers were then removed from the solution and dried under vacuum. To correct for charging, peak locations were referenced to the most intense carbon peak assumed to be present at 286.0 eV. This peak has previously been associated with the C−N bond.[1,2]

TEM analyses were performed using a JEOL 2010F microscope equipped with a Schottky field emission gun operated at 200 keV with an ultrahigh resolution pole piece providing a point resolution of 0.19 nm. Annular dark-field (ADF) imaging was completed using a 0.7 nm probe at a camera length of 20 cm. Samples were prepared using 200- or 300-mesh Cu grids coated with an ultrathin carbon film (Electron Microscopy Sciences, UltraThin carbon-coated Cu grids). Samples were prepared by placing a Cu grid onto filter paper, applying 1−5 drops of the appropriate Pt DEN solution, and allowing the specimen to dry in air.

EXAFS spectra were obtained at beamline X18B of the National Synchrotron Light Source at the Brookhaven National Laboratory. The samples were measured either in solution or dried to a powder and then dispersed on adhesive tape. The tape samples were then folded multiple times to ensure sample homogeneity. All samples were measured in transmission mode, and data analysis was subsequently completed using the IFEFFIT software package.[43]

High-energy XRD experiments were carried out at the 11-ID-B beamline (Advanced Photon Source, Argonne National Laboratory) using synchrotron radiation of 90.48 keV (λ = 0.1372 Å) at room temperature. Both wet and dry Pt DENs were measured. The scattered radiation was collected with a large-area detector (General Electric). The experimental XRD data were reduced to atomic PDFs using the function $G(r) = 4\beta r(\rho(r) - \rho_0)$, where $\rho(r)$ and ρ_0 are the local and average atomic number densities, respectively, and r is the radial distance.

Results and Discussion

UV−Vis Spectroscopic Analysis. Formation of the Pt^{2+}/dendrimer complex is the first step of the DEN synthesis. K_2PtCl_4 is usually the source of Pt^{2+}, but previous studies have shown that under most conditions it hydrolyzes in water.[5,44] To determine the form of Pt^{2+} that binds to the tertiary amine groups of the dendrimer, we carried out time-resolved UV−vis studies of the $PtCl_4^{2-}$ hydrolysis and the subsequent reaction between the dendrimer and Pt^{2+} (steps 1 and 2, Scheme 1). Recall that here Pt^{2+} represents any form of unreduced Pt^{2+}. Parts a−c of Figure 1 show time-resolved spectra obtained from 110, 294, and 480 μM aqueous $PtCl_4^{2-}$ solutions, respectively. These are the same concentrations used for the synthesis of 2.00 μM DEN solutions containing 55, 147, and 240 Pt atoms, respectively (vide infra).

Figure 1a confirms hydrolysis of $PtCl_4^{2-}$ present at the concentration used to prepare G6−OH$(Pt^{2+})_{55}$. The black spectrum, taken immediately after solution preparation, reveals absorbances at 215 and 230 nm, which are characteristic of $PtCl_4^{2-}$.[44] The intensity of these peaks decreases for ∼15 h and then achieves a nearly constant value (Figure 1d). The decrease in absorbance is directly attributable to the hydrolysis of $PtCl_4^{2-}$ to yield $PtCl_n(H_20)_{4-n}^{2-n}$ ($n \leq 3$).[44] Another important feature of these spectra is that at times >24 h, the absorbance at high wavelengths increases. We believe this is attributable to absorption and scattering of light associated with aggregation and/or polymerization of hydrolyzed $PtCl_n(H_20)_{4-n}^{2-n}$.[36] Indeed, a black precipitate is clearly observed after 72 h.

Spectra similar to those obtained for 110 μM are observed at 294 (Figure 1b) and 480 μM Pt^{2+} (Figure 1c). The initial and final (t > 20 h) absorbances of all three solutions (Figure 1d) scale approximately linearly with the initial concentration of $PtCl_4^{2-}$. The slight deviation from Beer's law is attributable to the overlapping

(42) Tokuhisa, H.; Zhao, M.; Baker, L. A.; Phan, V. T.; Dermody, D. L.; Garcia, M. E.; Peez, R. F.; Crooks, R. M.; Mayer, T. M. *J. Am. Chem. Soc.* **1998**, *120*, 4492–4501.

(43) Newville, M. *J. Synchrotron Radiat.* **2001**, *8*, 322–324.

(44) Elding, L. I.; Olsson, L. F. *J. Phys. Chem.* **1978**, *82*, 69–74.

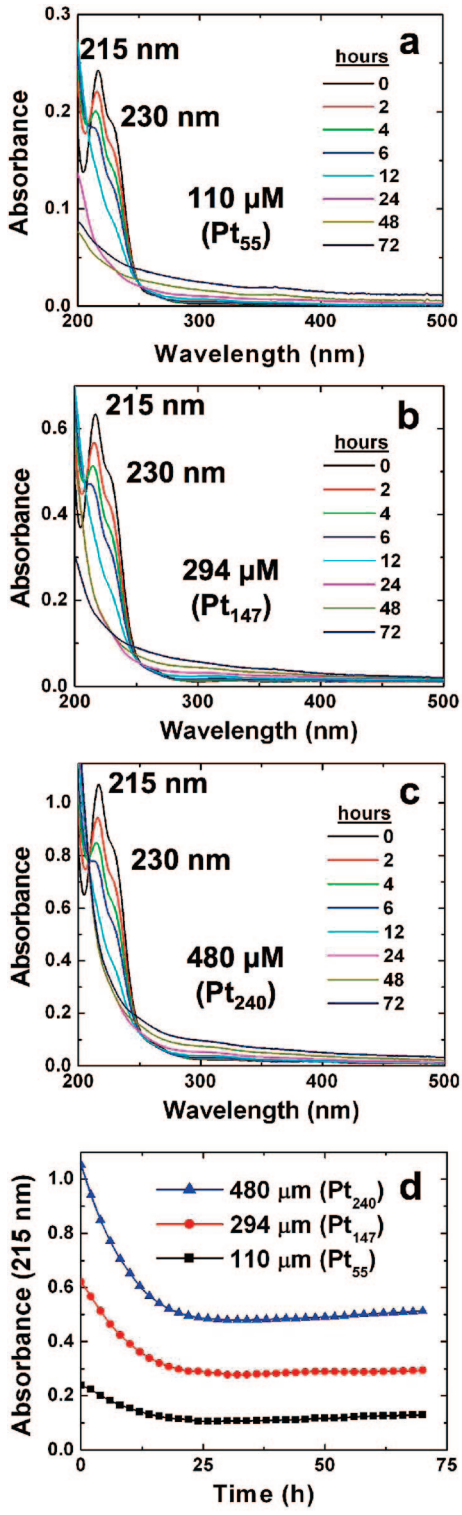

Figure 1. Time-resolved UV−vis spectra showing the hydrolysis of K_2PtCl_4 at concentrations of (a) 110, (b) 294, and (c) 480 μM, which represent the concentrations used for the synthesis of G6−OH(Pt_n), n = 55, 147, and 240, DENs, respectively. (d) Plots of the absorbance at λ = 215 nm (from parts a−c) as a function of time for the data shown in parts a−c. The reduction in the intensity of this peak corresponds to hydrolysis of $PtCl_4^{2-}$.

absorbance at 230 nm and the associated difficulty of accurately subtracting the background absorbance. Figure 1d indicates that the hydrolysis reaction reaches equilibrium within 20 h. From these data, a pseudo-first-order rate constant of 1.20×10^{-5} s^{-1} was determined. Details of this analysis are found in the Supporting Information (Figure S1). These kinetic results are reproducible and in good agreement with previous studies.[45,46]

In addition to studying the hydrolysis of $PtCl_4^{2-}$, we also carried out a spectroscopic study of the reaction between the G6−OH dendrimer and Pt^{2+}.[2,3,34] As discussed earlier, this is a two-step process in which $PtCl_4^{2-}$ first undergoes hydrolysis and then the hydrolysis product reacts with interior tertiary amines of the dendrimer to form a covalent bond (Scheme 1).[2,3,34,37,38,47,48] Figure 2a shows time-resolved spectra obtained during the preparation of G6−OH(Pt^{2+})$_{55}$. The first spectrum was obtained immediately after addition of an appropriate aliquot of freshly prepared, aqueous 10.0 mM K_2PtCl_4 to a 2.00 μM G6−OH dendrimer solution. As discussed earlier, the peaks at 215 and 230 nm are attributable to $PtCl_4^{2-}$.[44] These peaks decrease in intensity for approximately 10 h, at which time a peak at 250 nm begins to develop. This new band arises from the ligand-to-metal charge transfer (LMCT) from the tertiary amines of the dendrimer to bound Pt^{2+},[2,34,49] and it continues to grow for an additional 20 h. After a total of 30 h, the absorbance of the LMCT band achieves a nearly time-independent value (black curve, Figure 3a). As discussed later, there is no observable precipitation of zerovalent Pt metal when BH_4^- is added to Pt^{2+}/dendrimer solutions that have been allowed to react for 3 days, and therefore we conclude that the reaction between Pt^{2+} and the dendrimers is complete within this time period.

Parts b and c of Figure 2 provide time-resolved spectra for formation of the G6−OH(Pt^{2+})$_{147}$ and G6−OH(Pt^{2+})$_{240}$ complexes, respectively, and the corresponding changes in the LMCT bands are provided in Figure 3a (red and blue curves, respectively). These complexes, which have the highest Pt^{2+}/dendrimer ratios, exhibit LMCT bands having a slight ($\leq$2 nm) shift to higher wavelength. The increase in the steady-state absorbance of the three complexes is simply a consequence of the increasing Pt^{2+}/dendrimer ratio.

Figure 3b provides plots of the absorbance of the LMCT band as a function of time during the first 20 h of the reaction between Pt^{2+} and the dendrimers. The model (Scheme 1) predicts an induction period for the LMCT band corresponding to the time required for hydrolysis of $PtCl_4^{2-}$ (step 1), and this induction period is clearly observed in Figure 3b. The induction period, which is plotted in Figure 3c, is defined as the time required for a 1% increase in the initial absorbance at 250 nm. The induction period decreases as the Pt^{2+}/dendrimer ratio increases, because there is more hydrolyzed $PtCl_4^{2-}$ present in the more concentrated solutions at any specified time[50] and hence reaction with the dendrimer is detected sooner. From the experiments repre-

(45) Cotton, F. A.; Wilkinson, G.; Murillo, C. A.; Bochmann, M. *Advanced Inorganic Chemistry*; Wiley: New York, 1999.
(46) Tarazona-Vasquez, F.; Balbuena, P. B. *J. Phys. Chem. A* **2007**, *111*, 945–953.
(47) Zhang, Y.; Guo, Z.; You, X.-Z. *J. Am. Chem. Soc.* **2001**, *123*, 9378–9387.
(48) Baik, M.-H.; Friesner, R. A.; Lippard, S. J. *J. Am. Chem. Soc.* **2003**, *125*, 14082–14092.
(49) Fanizzi, F. P.; Intini, F. P.; Maresca, L.; Natile, G. *J. Chem. Soc., Dalton Trans.* **1990**, 199.
(50) Grantham, L. R.; Elleman, T. S.; Martin, D. S. *J. Am. Chem. Soc.* **1955**, *77*, 2965–2971.

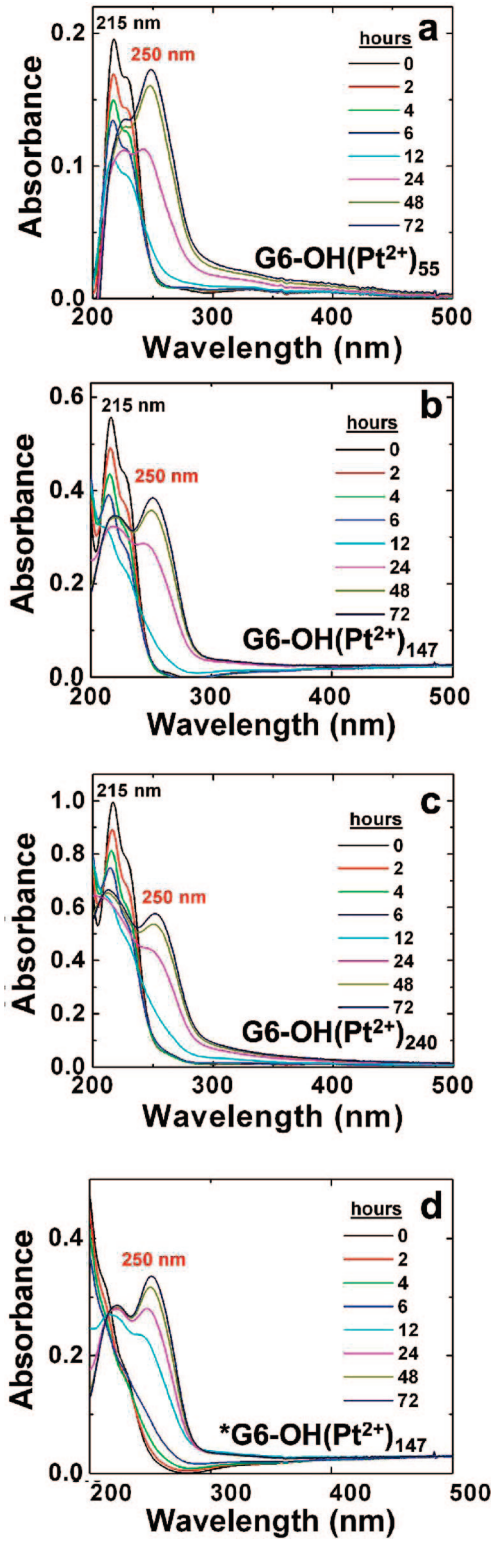

Figure 2. Time-resolved UV−vis spectra indicating formation of (a) G6−OH(Pt^{2+})$_{55}$, (b) G6−OH(Pt^{2+})$_{147}$, and (c) G6−OH(Pt^{2+})$_{240}$ complexes. A freshly prepared K_2PtCl_4 solution was used in parts a−c prior to mixing with the dendrimer solution. (d) Time-resolved UV−vis spectra for the synthesis of G6−OH(Pt^{2+})$_{147}$ using a K_2PtCl_4 solution prepared 12 h prior to complex formation.

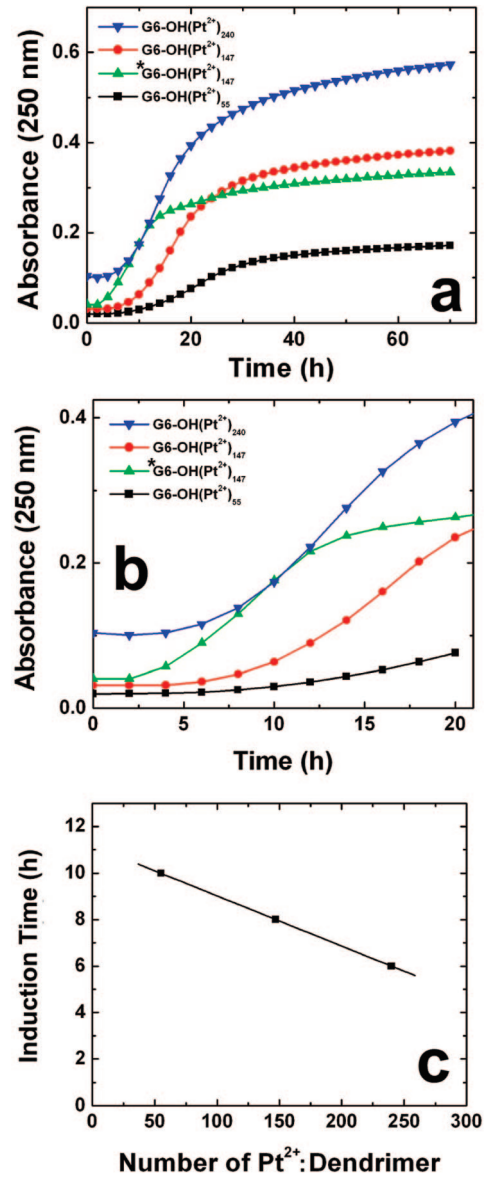

Figure 3. (a) Plots of the absorbance of the LMCT band ($\lambda = 250$ nm) for the Pt^{2+}/dendrimer complex as a function of time derived from the results shown in Figure 2. (b) Same as (a), except on an expanded time scale. (c) Plot of the induction time for formation of the Pt^{2+}/dendrimer complex as a function of the Pt^{2+}/dendrimer ratio. The induction time is defined as the time required for a 1% increase in the initial absorbance at $\lambda = 250$ nm.

sented by Figures 1–3, we can draw three important conclusions. First, $PtCl_4^{2-}$ must hydrolyze prior to reacting with the dendrimer. Second, formation of the complex is kinetically controlled and hence depends on the concentration of the hydrolyzed Pt^{2+} precursor in solution. Third, regardless of the Pt^{2+}/dendrimer ratio, reaction between $PtCl_n(H_2O)_{4-n}^{2-n}$ ($n \leq 3$) and G6−OH is complete within 30 h.

To confirm the validity of these three conclusions, three key control studies were carried out. The first experiment is represented by Figure 2d. Here, a 10.0 mM stock solution of K_2PtCl_4 was prepared, but it was allowed to hydrolyze for 12 h before it was mixed with the G6−OH solution. Notice that in this case, a small absorbance at 250 nm (corresponding to the Pt^{2+}/G6−OH complex) is observed after just 2 h (Figure 2d). The use of prehydrolyzed K_2PtCl_4 should eliminate the induction period observed for freshly prepared K_2PtCl_4 solutions, and the rate of complex formation should only be limited by the reaction between $PtCl_n(H_2O)_{4-n}^{2-n}$ ($n \leq 3$) and the dendrimer. Indeed, a comparison of the red (not prehydrolyzed) and green

(prehydrolyzed) curves in Figure 3, parts a and b, clearly indicates that formation of the Pt^{2+}/dendrimer complex occurs more quickly when $PtCl_4^{2-}$ is prehydrolyzed.

A second control experiment was carried out in which freshly prepared K_2PtCl_4 and G6−OH solutions were mixed in an effort to prepare G6−OH$(Pt^{2+})_{147}$, but this time 1.00 M KCl was also present. It is known that under these conditions the common-ion effect prevents hydrolysis of $PtCl_4^{2-}$.[45] Time-resolved spectra corresponding to this experiment are provided in the Supporting Information (Figure S2). No changes in these spectra are observed even after 72 h, confirming that no reaction takes place between Pt^{2+} and the dendrimer in the absence of $PtCl_4^{2-}$ hydrolysis (Scheme 1).

The third control experiment was intended to confirm that all, or nearly all, of the Pt^{2+} reacts irreversibly with the dendrimer. This experiment was carried out as follows. First, two solutions were prepared consisting of hydrolyzed $PtCl_4^{2-}$ and G6−OH$(Pt^{2+})_{147}$. Second, these solutions were passed through Millipore Centricon centrifugal filters having a molecular weight cutoff of 10 kDa. Third, the UV−vis absorbance spectra of the original solutions were compared to those of the filtrates. The resulting spectra are provided in the Supporting Information (Figure S3). For hydrolyzed Pt^{2+}, nearly all of the Pt^{2+} is recovered in the filtrate, but for the Pt^{2+}/dendrimer complex the amount of Pt^{2+} observed in the filtrate is below the detection limit. Accordingly, we conclude that all, or nearly all, Pt^{2+} is strongly associated with the dendrimer.

Following reaction of Pt^{2+} with the dendrimer, addition of $NaBH_4$ results in formation of DENs. The notation for the reduced DENs is G6−OH$(Pt)_n$ (n = 55, 147, or 240), but note that subscript n refers to the Pt^{2+}/G6−OH ratio used for the synthesis and is not meant to imply that each DEN has this exact composition. Figure 4a compares the UV−vis spectra of G6−OH$(Pt^{2+})_{55}$ before and after reduction. Reduction leads to two significant spectral changes. First, the LMCT band at 250 nm decreases, and second, there is an increase in absorbance at longer wavelengths.[51] As we have pointed out previously, these observations are consistent with only partial reduction of the Pt^{2+}/dendrimer complex.[2] These same observations apply to the G6−OH$(Pt^{2+})_{147}$ and G6−OH$(Pt^{2+})_{240}$ precursors. Unfortunately, it is not possible to obtain quantitative information about the extent of reduction from these spectra for the following two reasons. First, there is no way to prepare a 100% reduced solution of the Pt DENs (vide infra), and therefore it is not possible to determine the extinction coefficients of the pure compounds. Second, because of the extensive overlap of the spectra before and after reduction, there is no means to determine the background signal originating from the partially reduced DENs and hence the absorbance arising from just the unreduced precursor. Accordingly, it is not possible to accurately determine the percentage absorbance arising from the unreduced DENs at λ_{max} for the precursor. However, the extent of reduction can be extracted from the EXAFS data discussed later. One final point: we carried out a filtration

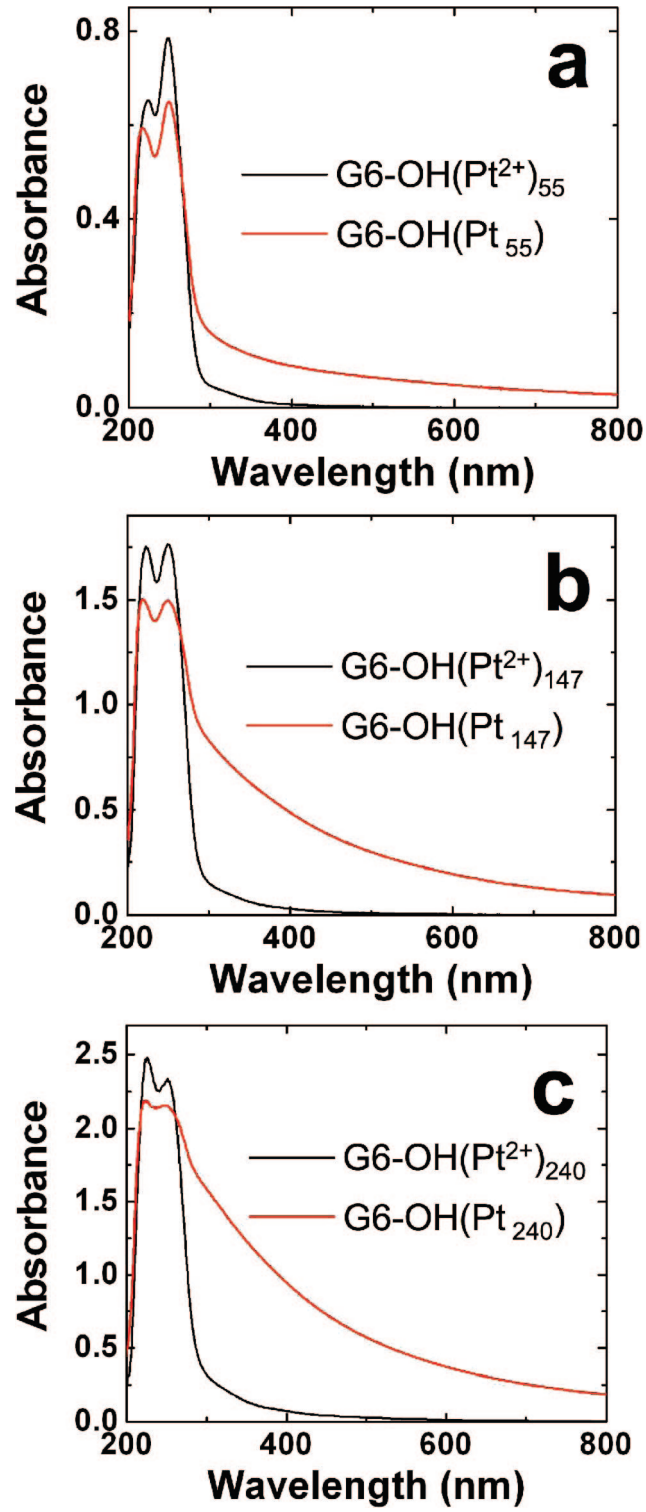

Figure 4. UV−vis spectra for the (a) G6−OH$(Pt^{2+})_{55}$, (b) G6−OH$(Pt^{2+})_{147}$, and (c) G6−OH$(Pt^{2+})_{240}$ complexes before and after reduction with BH_4^-. In all cases the G6−OH concentration was 10.0 μM, and $PtCl_4^{2-}$ was allowed to react with the dendrimer for 3.0 days prior to reduction.

experiment for G6−OH(Pt_{147}) like that described in the previous paragraph for G6−OH$(Pt^{2+})_{147}$ and found no detectable level of Pt^{2+} in the filtrate (Supporting Information, Figure S3). This experiment shows that even after reduction all forms of platinum are associated with the dendrimer.

(51) Creighton, J. A.; Eadon, D. G. *J. Chem. Soc., Faraday Trans.* **1991**, *87*, 3881–3891.

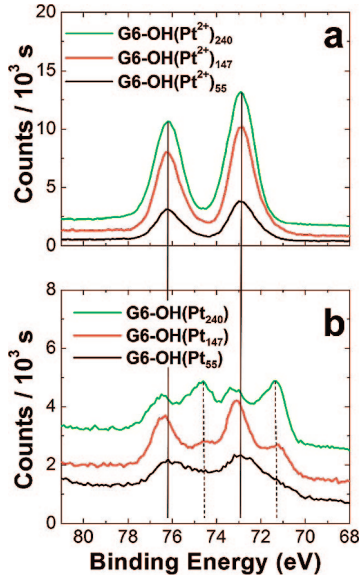

Figure 5. XPS spectra in the Pt(4f) region of the G6−OH$(Pt^{2+})_n$ complexes (a) before and (b) after reduction with BH_4^-.

X-ray Photoelectron Spectroscopy. XPS was used to confirm partial reduction of the Pt^{2+}/dendrimer complex. Before discussing the data, however, we wish to point out that there was a significant degree of charging in these samples, and therefore the positions of the Pt(4f) peaks were referenced to the location of the most intense carbon peak. The position of this peak (286.0 eV) was previously reported by Ozturk et al. for G4−OH PAMAM dendrimers, and therefore binding energies reported here can be directly compared to their results.[4] Nevertheless, the absolute binding energies reported here should be viewed with caution, although the relative shifts of the Pt(4f) peaks are reliable.

Figure 5a shows the Pt(4f) region of the unreduced complexes for the three Pt/G6−OH dendrimer ratios examined in this study. The Pt($4f_{7/2}$) peak lies at 72.9 eV for all three G6−OH$(Pt^{2+})_n$ complexes. This binding energy is close to the NIST database value of 73.4 eV reported for the $PtCl_4^{2-}$ starting material.[52] The slight shifts to lower binding energy observed for G6−OH$(Pt^{2+})_n$ are consistent with a strong LMCT interaction between Pt^{2+} and the dendrimer as EXAFS results have previously shown.[5] Note also that this binding energy is the same as we previously reported for G4−OH$(Pt^{2+})_{60}$[53] and close to that of several related Pt^{2+}−N complexes (73.1−73.5 eV).[54]

Pt is present in two distinct oxidation states after addition of BH_4^- (Figure 5b), confirming only partial reduction of the Pt^{2+}/dendrimer complexes. The positions of the pair of Pt($4f_{7/2}$) and Pt($4f_{5/2}$) peaks at higher binding energy closely correlate to the positions observed prior to reduction, but they are shifted very slightly to higher energy. This might suggest selective reduction of Pt^{2+} in specific metal-binding configurations within dendrimers, but the shift is so small that even this degree of speculation may be unwarranted.

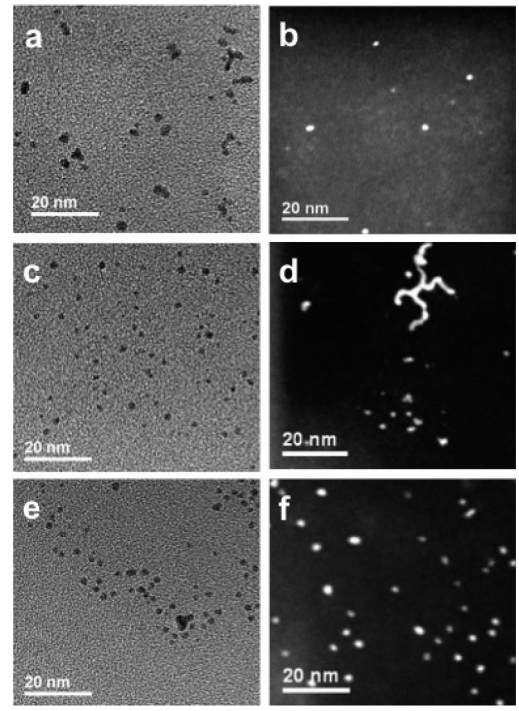

Figure 6. Representative BF micrographs of (a) G6−OH(Pt_{55}), (c) G6−OH(Pt_{147}), and (e) G6−OH(Pt_{240}), and (b), (d), and (f) the corresponding ADF micrographs, respectively.

The Pt($4f_{7/2}$) and Pt($4f_{5/2}$) peaks at lower binding energy presumably correspond to reduced Pt in the form of DENs. Regardless of the size of the DENs, the Pt($4f_{7/2}$) peak is present at 71.3 ± 0.1 eV which is consistent with the value for bulk Pt (71.2 eV).[52] Wang et al. reported a similar binding energy (71.4 eV) for nanoparticles of comparable size.[55] A previous study by Ozturk et al. reported the binding energy of the Pt($4f_{7/2}$) peak for a G4−OH(Pt_{40}) DEN monolayer at 73.3 eV.[4] We previously reported binding energies of 73.0 eV[2] and 71.3 eV[53] for G4−NH_2(Pt_{30}) and G4−OH(Pt_{60}) DENs, respectively. The absolute values for reduced Pt will depend on a number of factors, but the important result is that the XPS data clearly indicate just partial reduction of the Pt^{2+}/dendrimer precursor complex by BH_4^-.

TEM Analysis. Pt DENs nominally consisting of 55, 147, and 240 atoms were analyzed by TEM. Samples were prepared by applying several drops of a DEN solution onto a Cu grid coated with an ultrathin carbon film. Figure 6 shows representative bright-field (BF) and ADF micrographs of the Pt DENs at moderate magnifications. ADF imaging was used in addition to conventional BF imaging to provide enhanced *Z*-contrast for Pt, which significantly improved detection of the smallest nanoparticles. In all images, the majority of the nanoparticles have a nearly isometric morphology; however, there is a minority of agglomerated particles. At this time we are uncertain whether these structures exist in solution, or whether they form during drying prior to TEM analysis. Typical chain lengths are equivalent to 2−5 linearly aggregated nanoparticles, but occasionally long irregularly shaped chains are observed, such as that shown at the top of Figure 6d.

(52) Wagner, C. D.; Riggs, W. M.; Davis, L. E.; Moulder, J. F. *Handbook of X-Ray Photoelectron Spectroscopy*; Perkin-Elmer Corporation: Chanhassen, MN, 1995.
(53) Zhao, M.; Crooks, R. M. *Adv. Mater.* **1999**, *11*, 217–220.
(54) Matsumoto, K.; Sakai, K.; Nishio, K.; Tokisue, Y.; Ito, R.; Nishide, T.; Shichi, Y. *J. Am. Chem. Soc.* **1992**, *114*, 8110–8118.
(55) Wang, J. J.; Ying, G. P.; Zhang, J.; Wang, Z. B.; Gao, Y. Z. *Electrochim. Acta* **2007**, *52*, 7042–7050.

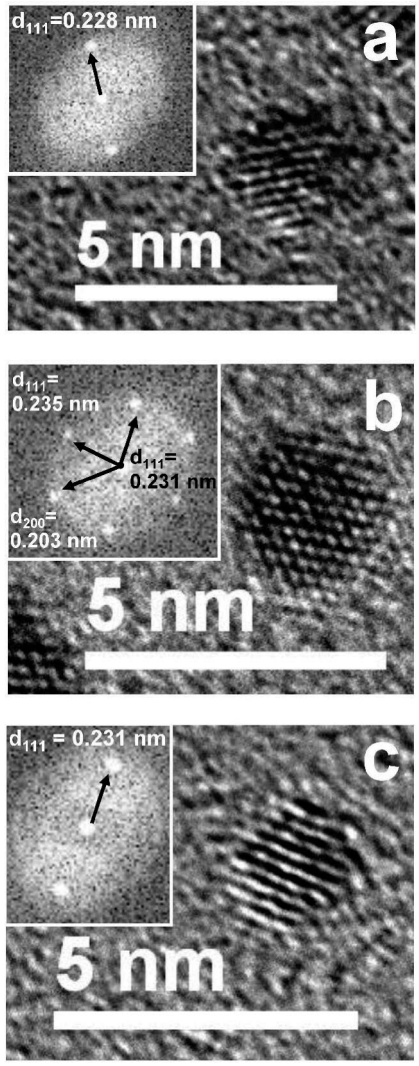

Figure 7. HREM micrographs of (a) G6−OH(Pt_{55}), (b) G6−OH(Pt_{147}), and (c) G6−OH(Pt_{240}). The insets show the FFT patterns for each particle and the measured *d*-spacing.

The measured sizes for the G6−OH(Pt_{55}), G6−OH(Pt_{147}), and G6−OH(Pt_{240}) DENs are 1.3 ± 0.3, 1.6 ± 0.3, and 2.0 ± 0.4 nm, respectively. The pixel resolution used for these measurements ranged between 0.05 and 0.25 nm and agglomerates were not counted. These values can be compared to the theoretical values for the diameters of cuboctahedral particles containing these same numbers of atoms: 1.2, 1.6, and 1.9 nm,[16] respectively. This high level of agreement is consistent with complete reduction of the Pt^{2+}/dendrimer precursors but contrary to the UV−vis and XPS results discussed earlier.

High-resolution electron microscopy (HREM) imaging of the reduced DENs clearly show that they are relatively well-ordered at the atomic scale. Figure 7 displays high-resolution images of all three DENs with their respective diffraction pattern obtained from fast Fourier transform (FFT) analysis. From this analysis (insets in Figure 7), characteristic interplanar spacings, *d*, between planes of Pt atoms inside DENs have been measured. The distances are found to be very close to interplanar spacing d_{111} = 2.27 Å and d_{200} = 1.96 Å observed in bulk fcc Pt.

One final point regarding the TEM analysis of Pt DENs: we were concerned that the electron beam itself might reduce the G6−OH(Pt^{2+})$_n$ DEN precursors. Accordingly, we examined grids prepared with the G6−OH(Pt^{2+})$_{147}$ complex, the G6−OH(Pt^{2+})$_{147}$ complex after reduction with BH_4^- for 2 h (to create Pt seeds that might catalyze further electron-beam-stimulated reduction), and the G6−OH(Pt^{2+})$_{147}$ complex after reduction with BH_4^- for 24 h every 5 min during a 1 h electron-beam exposure. This experiment is described in detail in the Supporting Information, and representative micrographs are provided (Figure S4). The result is that in all three cases no growth of Pt nanoparticles was observed for electron-beam exposure times up to 1 h. This time greatly exceeds that required to image Pt DENs (Figures 6 and 7) and leads to burning of the carbon grid. Accordingly, we conclude that under the conditions used to obtain the results reported here, the influence of the electron beam on the formation of DENs is negligible.

EXAFS Analysis. EXAFS studies were conducted on Pt DENs in the solid state and dissolved in water (DEN concentration = 100 μM), which we refer to as "dry" and "wet" DENs, respectively. This comparison provides an opportunity to determine how the presence of water might affect the DEN structure, extent of reduction, and stability.[5] The EXAFS analyses for dry and wet G6−OH(Pt_n) (n = 55, 147, and 240) DENs are provided in Figure 8, and the corresponding data for n = 100 and 200 (wet samples only) is given in the Supporting Information (Figure S5). In all cases, the black curves represent the experimentally obtained and Fourier-transformed EXAFS data and the red curves are the fits obtained using FEFF6 theory[56] and the Artemis analysis program.[57] Each data set was obtained as an average of four independent energy scans to improve the signal-to-noise ratio.

The important conclusion from the EXAFS study is that the experimentally determined CNs of the dry DENs are clearly related to the Pt^{2+}/dendrimer ratio used for the synthesis. Specifically, a Pt−Pt CN of 1.07 ± 0.55 was determined for the dry G6−OH(Pt_{55}) DENs (Figure 8a), which is quite low for a Pt particle consisting of 55 atoms. This observation indicates that only a small fraction of the total Pt^{2+} initially present in the G6−OH(Pt^{2+})$_{55}$ precursor solution is reduced. Indeed, we can estimate the percentage of Pt^{2+} ions that are reduced by comparing the experimental value of the CN (1.07) with the value calculated for a particle with a cuboctahedral shape consisting of 55 atoms (7.86).[58] This calculation reveals that only 14% of the total number of encapsulated Pt^{2+} ions are reduced during the preparation of G6−OH(Pt_{55}) DENs. However, EXAFS does not provide information on how the reduced fraction of Pt^{2+} is distributed between dendrimers. It may seem intuitive that each dendrimer would contain roughly equal numbers of reduced and unreduced Pt^{2+}, but the TEM results, and the XRD results discussed later, indicate this is not true. Rather, a minority of dendrimers contain fully reduced DENs (that is,

(56) Rehr, J. J.; Albers, R. C.; Zabinsky, S. I. *Phys. Rev. Lett.* **1992**, *69*, 3397–3400.
(57) Ravel, B.; Newville, M. *J. Synchroton Radiat.* **2005**, *12*, 537–541.
(58) Glasner, D.; Frenkel, A. I. *XAFS 13, Proc. Int. Conf. X-ray Absorpt. Fine Struct.* **2007**, *882*, 746–748.

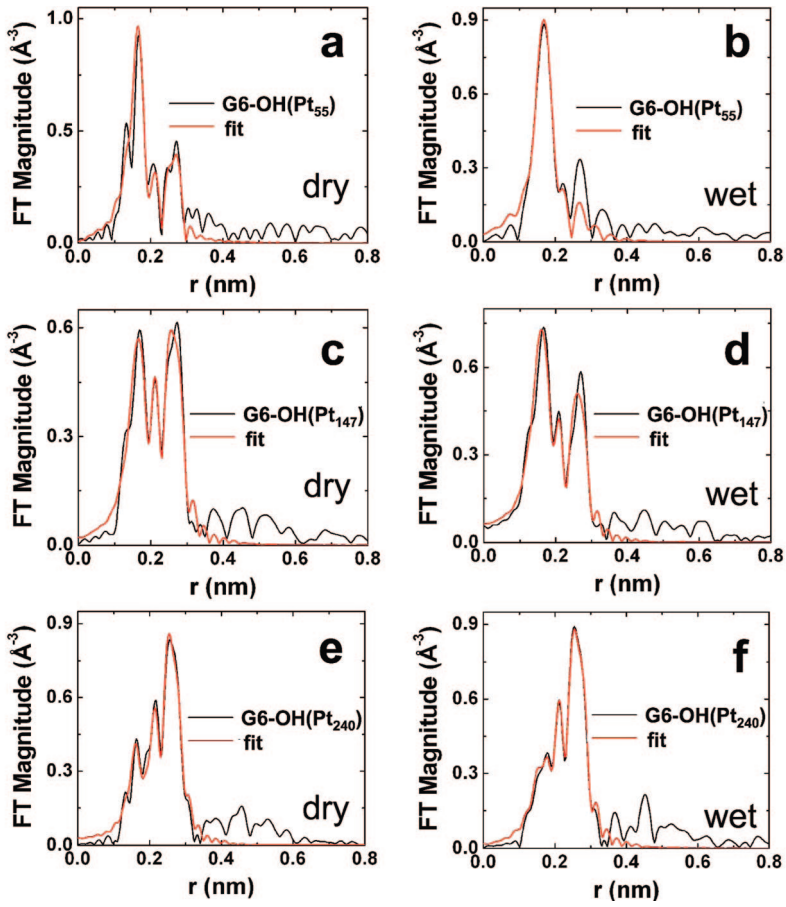

Figure 8. EXAFS analysis of (a and b) G6−OH(Pt_{55}), (c and d) G6−OH(Pt_{147}), and (e and f) G6−OH(Pt_{240}). The black curves represent the experimentally obtained data, and the red curves correspond to the calculated fits.

G6−OH(Pt_{55})) and a majority of dendrimers contain Pt^{2+} that is not reduced at all (that is, G6−OH(Pt^{2+})$_{55}$).

As the Pt^{2+}/G6−OH ratio increases to 147 and 240, the overall Pt−Pt CN increases to 3.99 ± 0.61 and 6.09 ± 0.42, respectively (the CNs for the dry DENs are plotted as a function of the Pt^{2+}/dendrimer ratio in Figure 9a). These values can be compared to theoretical Pt−Pt CNs for regular cuboctahedra of 8.98 and 9.52, respectively (Figure 9c).[58] With the use of the experimental and calculated values of the CNs, it is possible to use the approach discussed in the previous paragraph to estimate the fraction of encapsulated Pt^{2+} ions reduced by BH_4^- for the higher Pt^{2+}/G6−OH ratios. These values are 44% and 64% reduction of the total Pt^{2+} originally present in G6−OH(Pt^{2+})$_{147}$ and G6−OH(Pt^{2+})$_{240}$, respectively. Figure 9d is a plot of the percentage of Pt^{2+} reduced as a function of the Pt^{2+}/G6−OH ratio for all three Pt^{2+}/G6−OH ratios examined in this study. It shows that as the Pt^{2+}/G6−OH ratio increases, the total percentage of Pt^{2+} reduced increases. We will return to this observation later.

The trend in CNs for wet DENs (Figures 8, 9b, and Supporting Information Figure S2) is similar to that observed for the dry Pt DENs. Here, the Pt−Pt CNs are 0.39 ± 2.05, 2.86 ± 0.84, 3.38 ± 0.80, 6.25 ± 0.48, and 6.29 ± 0.38 for G6−OH(Pt^{2+})$_n$ (n = 55, 100, 147, 200, and 240, respectively). With the use of the same set of assumptions discussed in the previous two paragraphs, the percentage of reduced Pt can be calculated for the wet DENs. These values are 5%, 38%, and 66% for the G6−OH(Pt^{2+})$_n$ (n = 55, 147, 240) precursors, respectively. Within the uncertainty of the measurements, these values are very close to those obtained for the dry DENs: as the Pt^{2+}/G6−OH ratio increases, the percentage of Pt^{2+} reduced increases (Figure 9d).

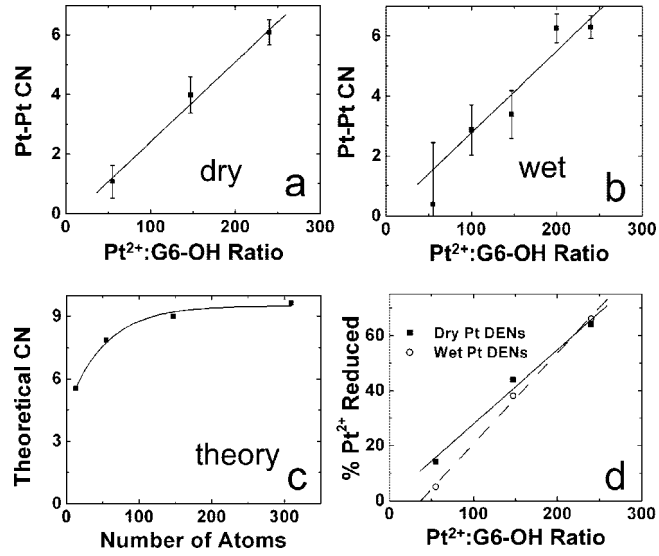

Figure 9. Comparison of the Pt−Pt CNs for (a) dry and (b) wet Pt DENs at the indicated Pt^{2+}/G6−OH ratios. (c) Calculated M−M CNs for cuboctahedral particles in this size range. (d) A plot of the percentage of Pt reduced as a function of the Pt^{2+}/G6−OH ratio.

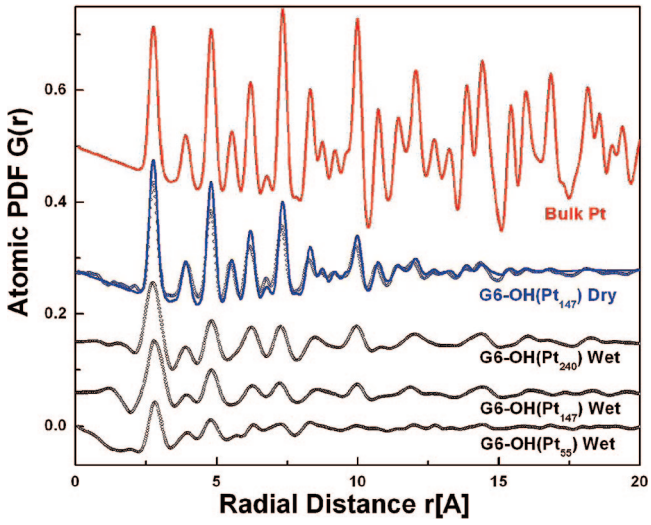

Figure 10. Experimental PDFs (symbols) for the indicated wet and dry Pt DENs. Model PDFs for bulk Pt (red plot) and a hypothetical 1.7 nm Pt particle with an fcc-type structure (blue plot) are also shown.

We attempted to induce a higher percentage of Pt^{2+} reduction by bubbling H_2 through the G6−OH(Pt_{100}) and G6−OH(Pt_{200}) solutions of wet DENs for 20 h after the initial EXAFS analysis. The fitting analyses of these data are provided in the Supporting Information (Figure S5). However, no change in the Pt−Pt CN is observed for either sample, indicating that no further reduction occurs for these DENs in the presence of a saturated, aqueous H_2 solution.

XRD/PDF Analysis. To better understand the structure of the Pt DENs, we performed high-energy XRD/PDF analyses[59] of the wet and dry Pt DENs. As shown in Figure 10, the PDF for bulk Pt exhibits well-defined peaks to high interatomic distances. This characteristic reflects the perfect fcc-type structure of crystalline metallic materials. Dry G6−OH(Pt_{147}) DENs exhibit similarly well-defined PDFs (sharp peaks), which indicate they are also crystalline and may be approximated in terms of a finite particle having an fcc-type lattice that is only moderately strained due to surface relaxation. Additionally, decay of the dry G6−OH(Pt_{147}) PDF indicates a correlation length of 1.7 nm (CN = 10), which is consistent with both the expected (1.6 nm) and measured (TEM: 1.6 ± 0.3 nm) values for the diameters of the G6−OH(Pt_{147}) DENs.

The experimental PDFs for wet Pt DENs resemble those of dry Pt DENs, but the plots are not as well-defined (broader peaks than for dry G6−OH(Pt_{147}) and bulk Pt). Also, the PDFs for wet DENs decay to zero at distances somewhat less than the average DEN size (0.9, 1.5, and 1.9 nm correlation lengths for the G6−OH(Pt^{2+})$_n$ (n = 55, 147, 240) wet DENs, respectively). Clearly, the atomic ordering in wet Pt DENs resembles that of an fcc-type structure, but they also exhibit considerable local structural distortions and/or strain. This may result in atomic ordering with a broken periodicity as we have previously discussed.[60]

There are two other very important points relating to the XRD/PDF analyses. First, we have previously shown that the size of Au DENs (G6−OH(Au_{147})) measured by TEM (1.7 nm) and XRD/PDF is fully consistent with CNs determined by EXAFS.[60] That is, the CNs determined by EXAFS for dry and wet G6−OH(Au_{147}) DENs were found to be 9.6 and 9.0, respectively, which are very close to the CNs calculated for a 147-atom regular cuboctahedron (8.98) and that determined by XRD/PDF for dry and wet G6−OH(Au_{147}) (9 ± 1). These results for Au DENs represent an important control experiment that unambiguously demonstrates that upon full reduction of all metal-ion/dendrimer complexes, TEM, EXAFS, and XRD/PDF yield identical results within the error limits inherent to these methods. This means that the differences in the EXAFS and XRD/PDF results measured for Pt DENs are real.

The second important point is that EXAFS measures the average CN for all metal atoms present in a sample: both Pt^{2+} and Pt^0. Therefore, the low CNs determined for the Pt DENs discussed here are consistent with partial reduction, but as mentioned earlier they do not provide information about the distribution of the reduced Pt. In contrast, and this is important, XRD/PDF is primarily sensitive to reduced Pt particles. Hence, taken together, the EXAFS and PDF data are fully consistent with a bimodal distribution of fully reduced Pt DENs and unreduced Pt^{2+}/dendrimer complexes. Interestingly, Figure 9d clearly shows that the extent of reduction depends on the loading of the dendrimer with Pt^{2+}: higher loadings yield a higher percentage of reduced Pt^{2+}.

Summary and Conclusions

We undertook this study to reconcile previous reports from our laboratory[2] and others[4,5] that dendrimer complexes with Pt^{2+} are not fully reduced when exposed to BH_4^- in aqueous solutions. We expected to discover that each dendrimer consisted of the same average number of reduced and unreduced Pt^{2+} complex ions. However, the use of five powerful analytical methods, UV−vis spectroscopy, XPS, TEM, EXAFS, and XRD/PDF, are consistent only with a model that invokes a bimodal distribution of reduced and unreduced intradendrimer Pt^{2+} (Scheme 1). Specifically, the UV−vis, XPS, and EXAFS data, which provide information about all Pt present within the sample regardless of its chemical state, indicate only partial reduction of G6−OH(Pt^{2+})$_n$. In contrast, TEM and XRD/PDF provide information only about reduced Pt^{2+} in the form of Pt nanoparticles. Because both TEM and XRD/PDF results reveal the presence of fully reduced DENs (that is, DENs having the correct size predicted based on the initial Pt^{2+}/G6−OH ratio used in the synthesis), we conclude that some dendrimers contain fully reduced DENs and some contain only Pt^{2+}. Importantly, TEM, EXAFS, and XRD/PDF studies carried out on Au DENs are internally self-consistent, and all three methods indicate the presence of fully reduced Au DENs.[60] This important set of control experiments instills confidence in the methodology used in the present study and the resulting conclusions.

(59) Egami, T.; Billinge, S. J. L. *Underneath the Bragg Peaks*; Pergamon Press: Amsterdam, 2003.
(60) Petkov, V.; Bedford, N.; Knecht, M. R.; Weir, M. G.; Crooks, R. M.; Tang, W.; Henkelman, G.; Frenkel, A. I. *J. Phys. Chem. C* **2008**, *112*, 8907–8911.

We are left to ponder the seemingly counterintuitive model that results from this study (Scheme 1). It may be reasonable to conclude that we are observing a stochastic, autocatalytic, intradendrimer nucleation and growth process. That is, for reasons we do not presently understand, BH_4^- is apparently capable of reducing Pt^{2+} complexed to the dendrimer via specific motifs.[36,46] Once reduction begins, however, it may become autocatalytic. That is, Pt^{2+} ions that are not directly susceptible to BH_4^- reduction may be catalytically reduced on the nascent Pt DEN. There is certainly ample prior evidence that Pt DENs are catalytic for hydrogenation reactions[28,34] and for decomposition of dendrimers,[4,61] which might support this hypothesis. Perhaps structural differences between dendrimers (that is, defect structures which are known to exist in PAMAM dendrimers to a substantial degree)[62] or different binding modalities between Pt^{2+} and the dendrimer[5,36] might account for this emergent heterogeneity. Certainly the data shown in Figure 9d, which shows that a higher percentage of Pt^{2+} is reduced in dendrimers having a higher loading of Pt^{2+}, is consistent with this view. That is, from a purely statistical viewpoint, higher loadings of Pt^{2+} provide more opportunities for a nascent Pt^0 nucleus to form.

Finally, we note that this bimodal reduction model is also consistent with our recently published study of the effect of Pt DEN size on the kinetics of the oxygen reduction reaction (ORR).[16] Specifically, this study indicated a monotonic trend in which smaller Pt particles resulted in slower ORR kinetics. This observation is more consistent with a bimodal distribution of Pt DEN catalysts that are fully formed (fully reduced), and hence catalytic, and a second distribution, which are unreduced and thus not catalytically active. If Pt within individual dendrimers was substantially present in multiple oxidation states, it is unlikely that catalytic activity approaching that of bulk Pt (for G6−OH(Pt_{240})) would have been observed because EXAFS indicates that such particles would have CNs on the order of 6. This CN corresponds to regular cuboctahedra consisting of just 13 atoms, which surely would have vastly different catalytic properties than bulk Pt.

(61) Singh, A.; Chandler, B. D. *Langmuir* **2005**, *21*, 10776–10782.
(62) Tomalia, D. A.; Baker, H.; Dewald, J.; Hall, M.; Kallos, G.; Martin, S.; Roeck, J.; Ryder, J.; Smith, P. *Polym. J.* **1985**, *17*, 117–132.

Acknowledgment. R.M.C. acknowledges support from the Robert A. Welch Foundation (Grant F-1288) and the National Science Foundation (Grant 0531030). Financial support of this project was also provided by the DOE-BES Grants DE-FG02-03ER15468 (R.M.C.), DE-FG02-03ER15468 (D.J.B.), and DE-FG02-03ER15476 (A.I.F.). Work at the NSLS was supported by DOE Grants DE-FG02-05ER15688 and DE-AC02-98CH10886, while work at the APS was supported by DOE contract W-31-109-ENG-38. V.P. acknowledges support from CMU through Grant REF 60628 and the help of Peter Chupas, APS, with the high-energy XRD measurements. M.R.K. and M.G.W. acknowledge the assistance of Ned Markinovich from NSLS for assistance with the EXAFS experiments. W.D.P. and D.J.B. acknowledge C. Ni and the UD Keck Microscopy facility for access to the JEOL 2010F and assistance with TEM. We acknowledge the Robert A. Welch Foundation and SPRING for support of some of the facilities used to carry out this project and Dr. Yangming Sun for assistance with the XPS measurements.

Supporting Information Available: Kinetic rate analysis of the $PtCl_4^{2-}$ hydrolysis reaction, UV−vis analysis indicating no hydrolysis of $PtCl_4^{2-}$ in the presence of 1.00 M KCl, spectroscopic evidence for complete sequestration of platinum within dendrimer, TEM results demonstrating that Pt^{2+} is not reduced under the electron beam, and EXAFS analysis of the wet G6−OH(Pt_{100}) and G6−OH(Pt_{200}) DENs before and after exposure to H_2 gas. This material is available free of charge via the Internet at http://pubs.acs.org.

CM8004198